

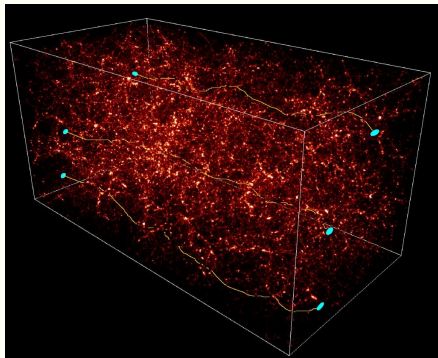
# Weak Gravitational Lensing by Galaxy Clusters and the Large Scale Structure

Jörg Dietrich

Douglas Clowe (OhioU)  
Jan Hartlap (AlfA)  
Lance Miller (Oxford)  
Norbert Werner (KIPAC)

Alexis Finoguenov (MPE)  
Tom Kitching (ROE)  
Aurora Simionescu (KIPAC)

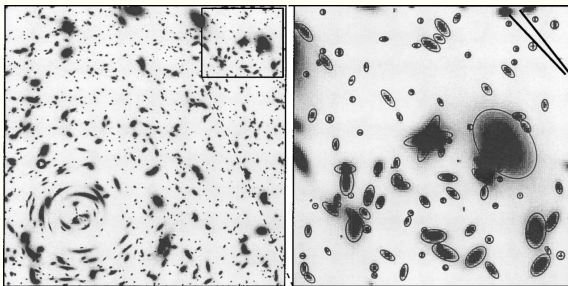
# The idea behind weak gravitational lensing



- ▶ Light from far away galaxies passes the large-scale structure (LSS).
- ▶ Gravitational lensing deflects the light bundles.
- ▶ The images of the background galaxies are distorted.

# What we measure in weak lensing

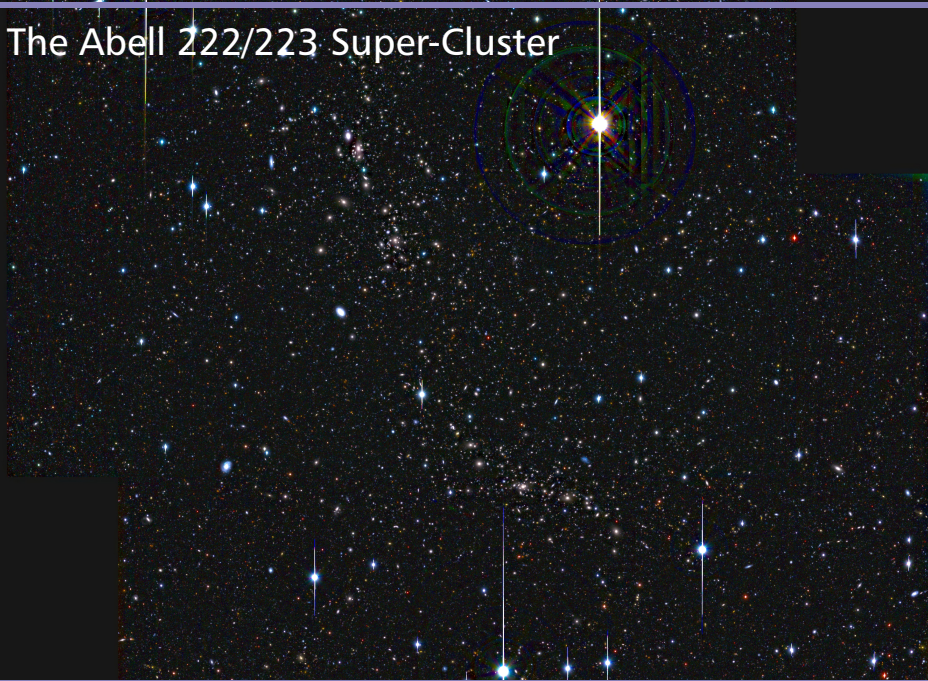
- ▶ Expectation value of intrinsic ellipticities vanishes,  $\langle \varepsilon^{(s)} \rangle = 0$
- ▶ In weak lensing shear is small,  $|\gamma| \ll 1$ :  $\varepsilon \approx \varepsilon^{(s)} + \gamma$
- ▶ Estimate the shear from observed ellipticities



Y. Mellier

- ▶ Then estimate the surface mass density  $\kappa$  from the shear.

# The Abell 222/223 Super-Cluster



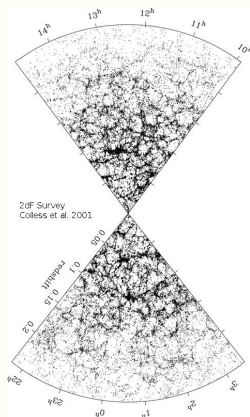


# The Abell 222/223 Super-Cluster

Dietrich et al. (2002, 2005):

- ▶ Separated by  $14'$  or  $2.8 \text{ Mpc}$
- ▶ A 222 at  $z = 0.213$ , A 223 at  $z = 0.208$ .
- ▶ If no peculiar velocity: Radial distance  $15 \text{ Mpc}$ .
- ▶  $M_{200}(\text{A222}) = 3.0^{+0.7}_{-0.8} \times 10^{14} M_{\odot}$ ,  
 $M_{200}(\text{A223}) = 5.3^{+1.6}_{-1.4} \times 10^{14} M_{\odot}$

# A 222/223 and the Cosmic Web

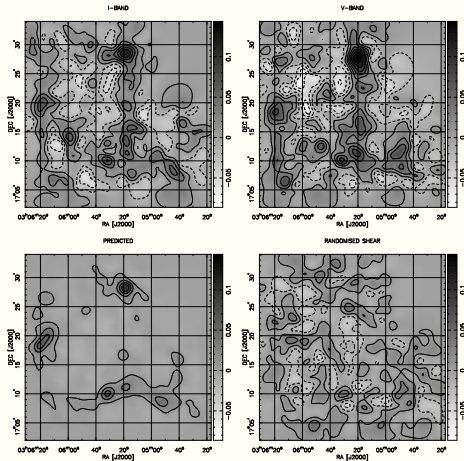


- ▶ Matter collapses into sheets and filaments.
- ▶ Filaments observed in redshift surveys.
- ▶ Filaments are where galaxies are transformed.
- ▶ Half of the local baryons are thought to reside in filaments (missing matter, WHIM).

We would like to see the total matter distribution. But finding filaments with weak lensing is hard . . .

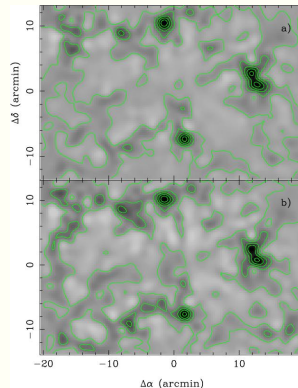
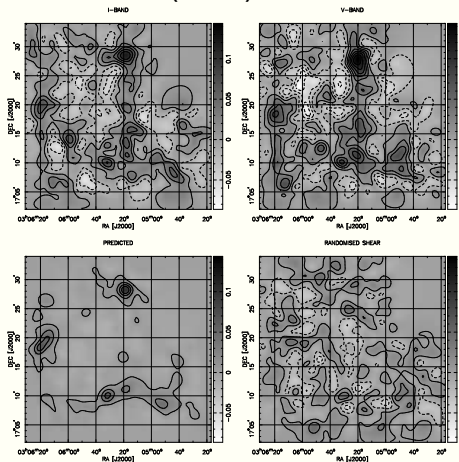
# The first candidate

Kaiser et al. (1998) in the MS 0302+17 system ( $z = 0.42$ ):



# The first candidate

Kaiser et al. (1998) in the MS 0302+17 system ( $z = 0.42$ ):

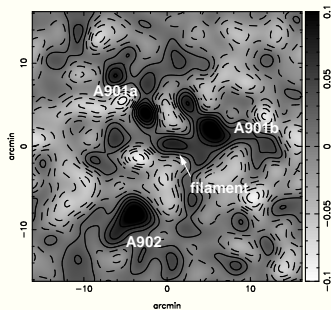


Gavazzi et al. (2004)

# The second candidate

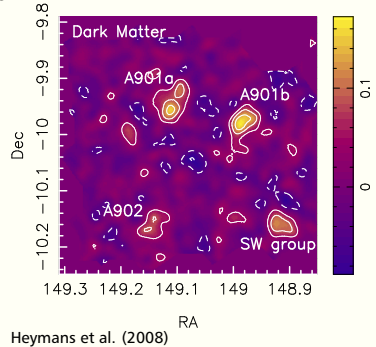
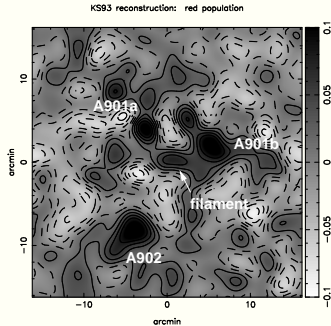
Gray et al. (2002) in the A 901/902 system ( $z=0.165$ ):

KS93 reconstruction: red population



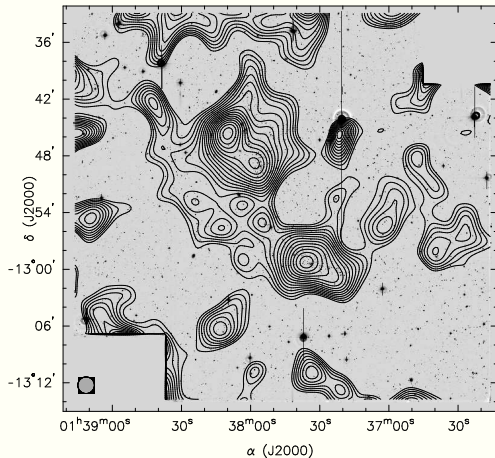
# The second candidate

Gray et al. (2002) in the A 901/902 system ( $z=0.165$ ):



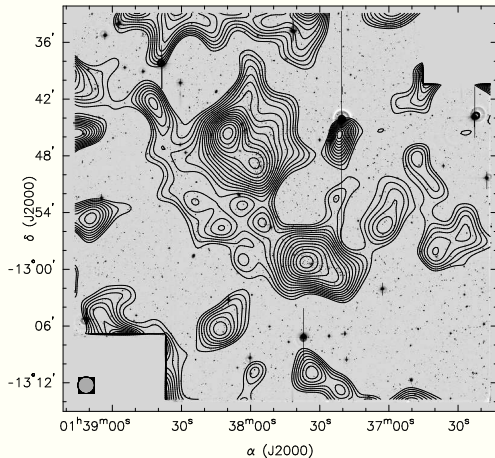
# The third candidate

Dietrich et al. (2005) in the A 222/223 system:



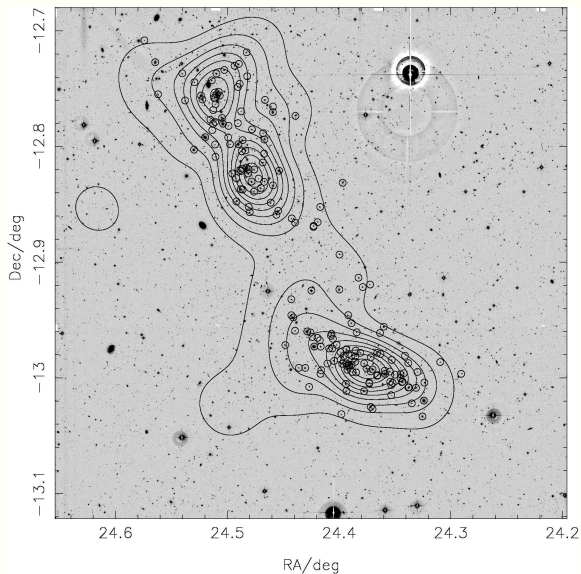
# The third candidate

Dietrich et al. (2005) in the A 222/223 system:





# Further evidence I



# Further evidence II

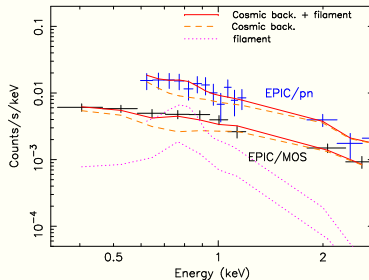
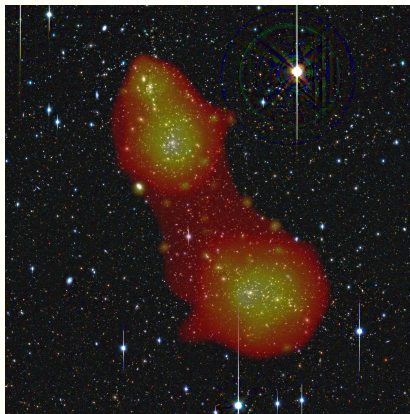
A&A 482, L29–L33 (2008)  
DOI: 10.1051/0004-6361:200809599  
© ESO 2008

**Astronomy  
&  
Astrophysics**

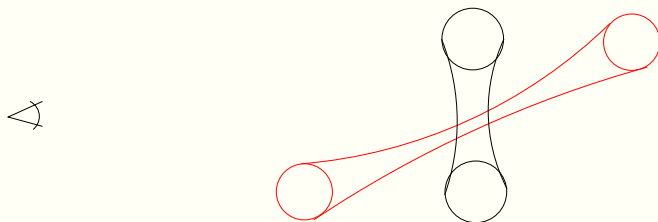
LETTER TO THE EDITOR

## Detection of hot gas in the filament connecting the clusters of galaxies Abell 222 and Abell 223

N. Werner<sup>1</sup>, A. Finoguenov<sup>2</sup>, J. S. Kaastra<sup>1,3</sup>, A. Simionescu<sup>2</sup>, J. P. Dietrich<sup>4</sup>, J. Vink<sup>3</sup>, and H. Böhringer<sup>2</sup>

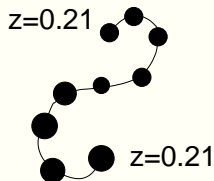


# Geometry is important



- ▶ Is the redshift difference a cosmological difference or peculiar velocities?
- ▶ Looking along the major axis could boost the surface mass density to a detectable level.

# A Timing Argument

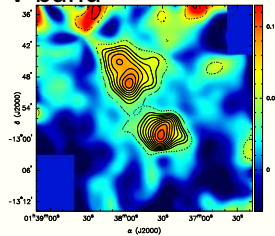


- ▶ Assume both cluster at the same point at  $z = \infty$ .
- ▶ Range of total system mass and inclination to reproduce  $\Delta z$  and  $\Delta\theta$ .
- ▶ Degeneracy between total mass and inclination.
- ▶ Smallest mass without redshift component:  
 $2.86 \times 10^{15} M_{\odot}$ , inclination 46 deg.

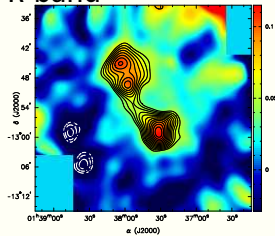
$\Rightarrow \Delta z$  is not peculiar velocity alone.

# New Mass Reconstructions

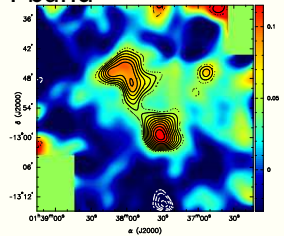
V-band



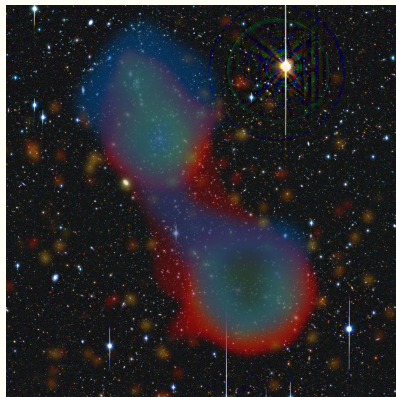
R-band



I-band



# Combining with X-ray



- ▶ X-ray and DM filament aligned.
- ▶ Gas mass inside circular  $1'6$  aperture:  
 $1.8 \times 10^{13} (l/15 \text{ Mpc}) M_{\odot}.$
- ▶ Lensing mass in same aperture:  
 $(1.5 \pm 0.3) \times 10^{14} M_{\odot}.$
- ▶ Hot gas fraction: 0.12.

# Summary – Part I

- ▶ A 222/3 is a supercluster at  $z = 0.21$ .
- ▶ Its main components are connected by a LSS filament.
- ▶ Clearly seen in galaxy distribution.
- ▶ Strong evidence for presence of WHIM from X-ray data.
- ▶ Best (only) weak-lensing candidate for filament detection.
- ▶ Physical parameters match expectations.

# Cosmic Shear



# How to constrain cosmology with weak lensing

The projected matter power spectrum is related to the 3-d power spectrum

$$P_{\kappa}(l) = \frac{9H_0^4 \Omega_m^2}{4c^4} \int_0^{w_m} dw \frac{g^2(w)}{a^2(w)} P_{\delta}\left(\frac{l}{w}, w\right)$$

Projected power spectrum

3-d matter power spectrum

# How to constrain cosmology with weak lensing

The projected matter power spectrum is related to the 3-d power spectrum

$$P_{\kappa}(l) = \frac{9H_0^4\Omega_m^2}{4c^4} \int_0^{w_m} dw \frac{g^2(w)}{a^2(w)} P_{\delta}\left(\frac{l}{w}, w\right)$$

direct dependence on cosmological parameters

# How to constrain cosmology with weak lensing

The projected matter power spectrum is related to the 3-d power spectrum

$$P_{\kappa}(l) = \frac{9H_0^4\Omega_m^2}{4c^4} \int_0^{w_m} dw \frac{g^2(w)}{a^2(w)} P_{\delta}\left(\frac{l}{w}, w\right)$$

redshift-distance relation

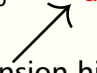
(includes galaxy redshift distribution)

# How to constrain cosmology with weak lensing

The projected matter power spectrum is related to the 3-d power spectrum

$$P_{\kappa}(l) = \frac{9H_0^4\Omega_m^2}{4c^4} \int_0^{w_m} dw \frac{g^2(w)}{a^2(w)} P_{\delta}\left(\frac{l}{w}, w\right)$$

expansion history




# How to constrain cosmology with weak lensing

The projected matter power spectrum is related to the 3-d power spectrum

$$P_{\kappa}(l) = \frac{9H_0^4\Omega_m^2}{4c^4} \int_0^{w_m} dw \frac{g^2(w)}{a^2(w)} P_{\delta} \left( \frac{l}{w}, w \right)$$

growth of structure

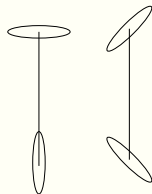


# How to constrain cosmology with weak lensing

We cannot measure projected mass directly. We measure galaxy ellipticities (shear).

The shear correlation functions

$$\xi_{\pm}(\theta) = \langle \gamma_t \gamma_t \rangle(\theta) \pm \langle \gamma_{\times} \gamma_{\times} \rangle(\theta)$$

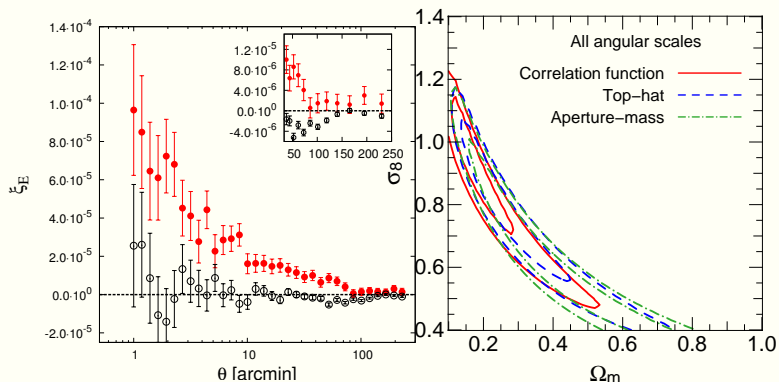


are related to the projected power spectrum

$$\xi_{+} = \int_0^{\infty} \frac{dl}{l} J_0(l\theta) P_{\kappa}(l) ; \xi_{-} = \int_0^{\infty} \frac{dl}{l} J_4(l\theta) P_{\kappa}(l)$$

This is what we measure in cosmic shear.

# Results from the CFHTLS



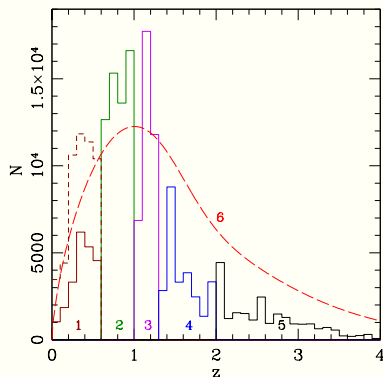
(Fu et al. 2008)

Degeneracy in  $\Omega_m$  and  $\sigma_8$ .

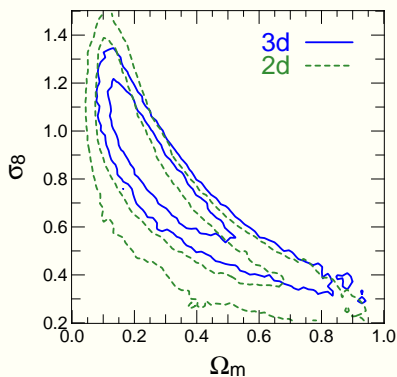
# Cosmic Shear tomography

Dividing the galaxies in redshift bins one can compute the auto- and cross-correlation functions

$$\xi_{\pm}^{(ij)}(\theta) = \langle \gamma_t^{(i)} \gamma_t^{(j)} \rangle(\theta) \pm \langle \gamma_{\times}^{(i)} \gamma_{\times}^{(j)} \rangle(\theta)$$



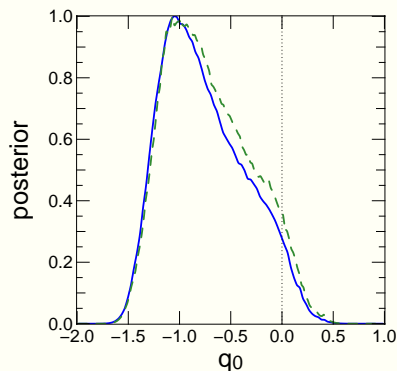
(Schrabback et al. 2010)



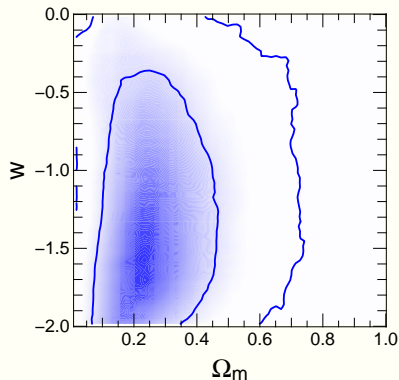


# More results from the COSMOS field

Evidence for accelerated expansion from cosmic shear:

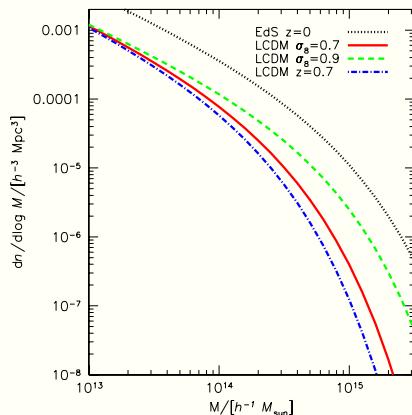


(Schraback et al. 2010)



# Beyond 2-point statistics

# Cosmology with the Mass Function

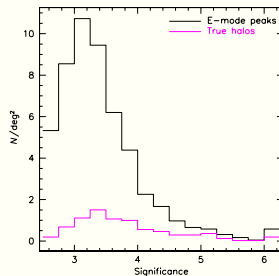


- Evolution of cluster mass function is cosmological probe.
- Clusters probe the non-linear (non-Gaussian) regime of structure formation.

Takada & Bridle (2007) showed that cluster cosmology and cosmic shear are complementary probes for dark energy.

# Weak Lensing Searches

- ▶ Weak lensing searches for galaxy clusters will always be incomplete, except at the highest masses (Hamana et al. 2004).
- ▶ Weak lensing searches will always have false positives from projections of LSS. These projections occur with all significances.



Dietrich et al. (2007)

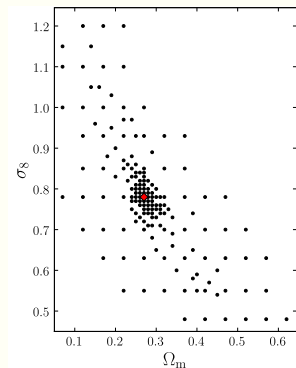
# The Peak Statistics

- ▶ At low SNR false positives are mainly caused by shape noise; at high SNR peaks are due to projections of large-scale structure.
- ▶ The weak lensing peaks caused by LSS are false positives only if one searches for galaxy clusters.
- ▶ LSS peaks caused by real mass along the line of sight.
- ▶ LSS peaks caused by real structure, part of the power spectrum.
- ▶ LSS peaks contain cosmological information.

Problem: Filaments and sheets are not collapsed structures.  
How do we predict the number of peaks as a function of cosmology?

# $N$ -body simulations

Make many  $N$ -body simulations for various cosmological parameters and ray-trace through them.



- ▶ 200  $N$ -body simulations in the  $\Omega_m$ - $\sigma_8$  plane.
- ▶ 166 different cosmologies ( $\Omega = 1$ ).
- ▶ 35 simulations at the fiducial cosmology (0.27, 0.78).
- ▶ Each simulation:  $256^3$  particles, 200 Mpc box (like GIF).
- ▶ Big enough to give  $10^{15} M_\odot$  halos.

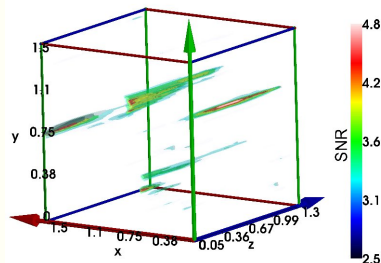
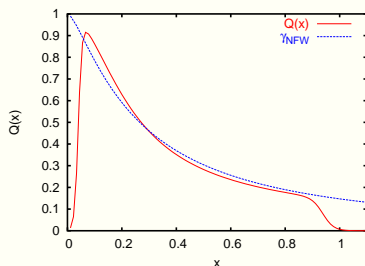
From each simulation: simulate five  $6 \times 6 \text{ deg}^2$  fields.  
CFHTLS like survey.

# Peak Finder

Aperture mass,  $M_{\text{ap}}$ ,

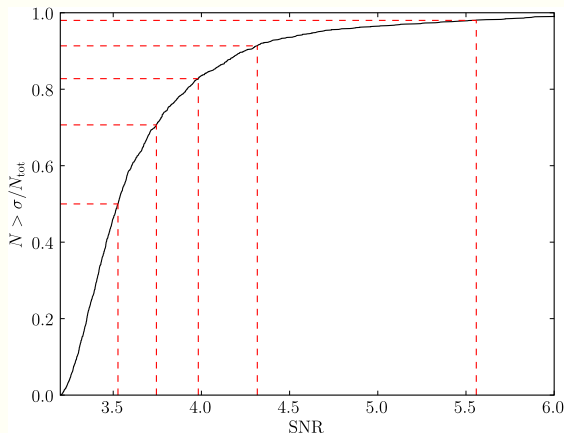
$$M_{\text{ap}}(\vec{\theta}_0) = \int d^2\theta Q(|\vec{\theta} - \vec{\theta}_0|) \gamma_t(\vec{\theta}; \vec{\theta}_0) ,$$

is a matched filter for shear if filter  $Q(\vartheta)$  follows expected shear profile.



# Signal-to-noise ratio data vector

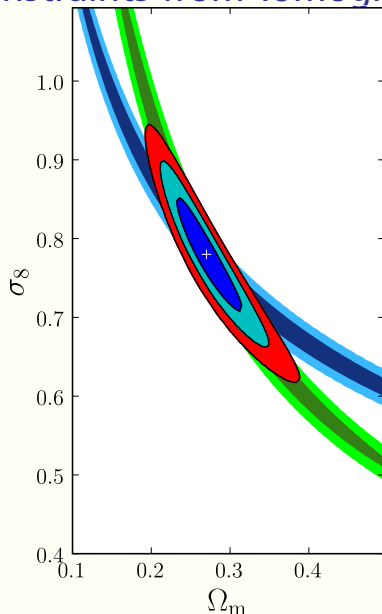
- ▶ We used SNR as a proxy for mass.
- ▶ Instead of using SNR bins, we take the cumulative SNR distribution.



With  $n$  logarithmically spaced bins:  $\vec{S}(\vec{\pi}) : \mathbb{R}^2 \rightarrow \mathbb{R}^n$

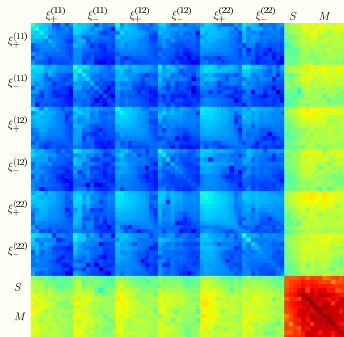


# Constraints from Tomographic Peaks



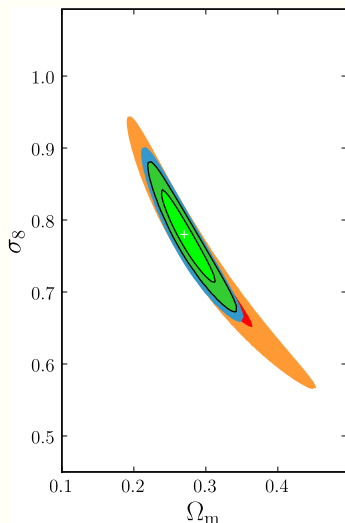
- ▶ Green contours are constraints from counting peaks per redshift bin.
- ▶ Blue contours are derived using the SNR distribution of peaks.
- ▶ Red/cyan/blue contours are the combination of both methods.
- ▶ Cannot use full  $N(\sigma, z)$  because covariance is limited.

# Combined covariance



- ▶ Cosmic shear and peak counts both measure the same density field.
- ▶ Significant cross-covariance between both methods expected.
- ▶ Cosmic shear tomography with 2 redshift bins and 10 spatial bins from  $30''$  to  $6$  deg.

# Combined constraints



- ▶ Both methods have very similar degeneracies.
- ▶ The peak statistics give competitive constraints.
- ▶ The combination of both methods further improves constraints.
- ▶ This is probably due to the inclusion of non-Gaussian fluctuations.

Type	Figure of Merit
Cosmic shear	71
Peak statistics	123
Combined	173

## Summary – Part II

- ▶ Peak statistics can constrain  $\Omega_m$ ,  $\sigma_8$  with projected peaks containing cosmological information.
- ▶ Peak tomography gives constraints which are competitive with cosmic shear tomography.
- ▶ The combination of both improves constraints.
- ▶ Application to surveys challenging at the moment. Emulators may be a solution.
- ▶ What about other parameters, Dark Energy?

# Summary

